JOURNAL OF SYNCHROTRON RADIATION
ISSN 1600-5775

Dynamic pulse-to-pulse thermal load effects in pulse-train-mode self-seeded X-ray free-electron laser

Zhengxian Qu,[a,b] Yanbao Ma,[b] Guanqun Zhou[a] and Juhao Wu[a]*

[a]SLAC National Accelerator Laboratory, Menlo Park, CA 94025, USA, and [b]Department of Mechanical Engineering, University of California Merced, Merced, CA 95343, USA. *Correspondence e-mail: jhwu@slac.stanford.edu

Received 4 December 2019
Accepted 29 August 2020

Edited by A. Momose, Tohoku University, Japan

Keywords: self-seeding free-electron laser; crystal monochromator; thermomechanical effects; high repetition rate; tuning process.

Thermal load has been a haunting factor that undermines the brightness and coherence of the self-seeded X-ray free-electron laser. Different from uniformly pulsed mode, in pulse train mode a thermal quasi-steady state of the crystal monochromator may not be reached. This leads to a dynamic thermal distortion of the spectral transmission curves and seed quality degradation. In this paper, the pulse-to-pulse thermal load effects on the spectral transmission curves and seed quality are shown, and some instructive information for the tuning process is provided.

1. Introduction

The free-electron laser (FEL) opens the door to a new frontier of various research fields, *e.g.* physics (Young *et al.*, 2010), chemistry (Zhang *et al.*, 2014), life (Seibert *et al.*, 2011) and material sciences (Milathianaki *et al.*, 2013). Combined with ultra-short duration, refined resolution, and high photon peak power, hard X-ray FELs have become powerful tools to capture simultaneous information of the atomic structure and dynamics, which have been exemplified by the successful operation of various X-ray FEL sources (Emma *et al.*, 2010; Ishikawa *et al.*, 2012; Kang *et al.*, 2017; Scholz, 2018), *e.g.* Linac Coherent Light Source (LCLS). The process of X-ray generation in these machines is based on self-amplified spontaneous emission (SASE) (Kondratenko & Saldin, 1980; Bonifacio *et al.*, 1984), in which the electron beam's spontaneous undulator emission is amplified during the continuous interaction when the electron beam travels through the undulator sections. The X-rays produced in the SASE process are transversely coherent. However, due to the stochastic nature of this process, the photons so generated have a temporal coherent duration much shorter than the entire electron bunch duration. Therefore the photons will not be all in a narrow bandwidth (Andruszkow *et al.*, 2000; Wu *et al.*, 2010; Zhou *et al.*, 2019).

One effective way to improve the X-ray temporal properties is the self-seeding technique, which has been demonstrated experimentally at LCLS (Amann *et al.*, 2012). With an inserted monochromator in the undulator system, the SASE FEL spectrum is filtered and a narrow-bandwidth wake seed is generated (Geloni *et al.*, 2011). Then, the narrow-bandwidth seed will be amplified in the later undulator segments. An alternative method to achieve hard X-ray self-seeding is to implement a reflective two-bounce monochromator, as successfully demonstrated at SACLA (Inoue *et al.*, 2019). In this way, the self-seeding scheme improves the FEL spectrum-brightness dramatically. Naturally, the 'seed' property has a

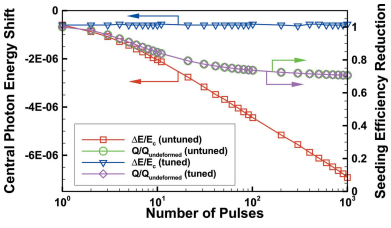

strong dependence on the monochromator properties, *e.g.* the material, the atomic reflection layer, lattice deformation field (bending, thermal deformation, *etc.*). Next-generation FEL facilities, like European XFEL, LCLS-II (Scholz, 2018; Emma *et al.*, 2014; Raubenheimer *et al.*, 2014) and LCLS-II-HE (Raubenheimer, 2016, 2018), are employing superconducting technology to improve the repetition rate (X-ray pulse per second) to the MHz level, to speed up the scientific discoveries utilizing the FEL pulses. Alongside these advances, these high-repetition-rate machines will bring new challenges on the thermal management of the self-seeding monochromator. Due to the ultra-short duration of FEL pulses, the self-seeding monochromator would be heated up instantaneously. This sudden temperature change will induce local strain and elastic waves. For a low repetition machine, there is enough time for the monochromator to recover; but for the high repetition machines, there will not be enough relaxation time before the next FEL pulse. Strain and surface slope field induced by this thermal effect would lead to seed property degradation, *e.g.* central photon energy shift, bandwidth broadening and seed pulse energy reduction.

With regard to this issue, studies on thermal load reduction and cooling have been carried out (Liu *et al.*, 2019; Samoylova *et al.*, 2019). In addition to thermal load reduction, it is also suggested that tuning the monochromator with a pitch oscillator (Liu *et al.*, 2019) can achieve better tolerance of the temperature increase. The implementation of the pitch oscillator actually raises a further question: how should the pitch angle (glancing angle for LCLS, EuXFEL and PAL-XFEL) of the monochromator be adjusted to yield better protection against the seed quality degradation? In this study, we provide some implications from the simulation perspective for the self-seeding operation in a pulse train mode, where the crystal periodically receives a train of pulses at a high repetition rate and relaxes for some time (Liu *et al.*, 2019). For reflective hard X-ray configuration as in SACLA, the analysis is more complicated due to multiple reflections. For simplicity, we focus on the transmissive self-seeding configuration as implemented in LCLS, LCLS-II, LCLS-II-HE, EuXFEL and PAL-XFEL, but similar analysis is also applicable for reflective configuration. We show the dynamic change of the seed quality including the transient behavior of the seed central photon energy shift and seeding efficiency (the pulse energy ratio between the seed and the incident SASE) reduction when a quasi-steady state is not reached. We accordingly address how the monochromator pitch angle should be adjusted and the pros and cons of this tuning method.

2. Simulation method

In this section, we briefly present the simulation details. The simulation tool can be divided into three interconnected modules: diffraction, thermal, and mechanical. The diffraction module was developed as an in-house MATLAB script based on Shvyd'ko's response function method (Shvyd'ko & Lindberg, 2012). The thermal and mechanical modules were based on the commercial finite-element analysis software *COMSOL*. During the simulation process, the diffraction module was implemented first to obtain the seed quality and the absorptance of the crystal. The absorptance then was imported as an input into the thermal and mechanical module, where the quasi-static strain and displacement field was simulated and exported back to the diffraction module to assess the seed quality of the next XFEL pulse. More details of the simulation module can be found in our previous work (Qu *et al.*, 2020*a*; Qu, 2020)

To evaluate the thermal load effects on the hard X-ray self-seeding, we choose a typical set of parameters: the SASE central photon energy is selected as 8.3 keV with 3 μJ pulse energy, 1.2×10^{-3} relative bandwidth, 40 μm (FWHM) spot size and 4.54 MHz repetition rate (Liu *et al.*, 2019). The diamond crystal monochromator is in (4 0 0) reflection of (1 0 0)-plane surface crystal with geometry specified by Dong *et al.* (2017). At the clamped edge of the crystal, the temperature is assumed to remain at environment temperature of 300 K due to cooling of the base holder. The cooling due to radiation emission from the crystal is neglected due to low crystal temperature. In total, 1000 pulses are simulated.

3. Results and discussions

Fig. 1 presents the temperature rise at the center of the SASE spot. Following the same terminology as in Liu *et al.* (2019), the pulsed results and quasi-continuous results (for validation only) are plotted and compared. Both curves capture the accumulated thermal load as more pulses arrive, and both curves indicate that a quasi-steady state, where pulse-to-pulse variation diminishes, has not been reached after 1000 pulses. Therefore, the thermal load is dynamic and varies with time, or number of pulses.

Accordingly, the seed quality is dynamic and varies from pulse to pulse as shown in Fig. 2. The central photon energy is normalized by the central photon energy of the spectral transmission curve of a perfect crystal. The seeding efficiency is also normalized by the seeding efficiency of a perfect crystal. Both the normalized seed central photon energy and the

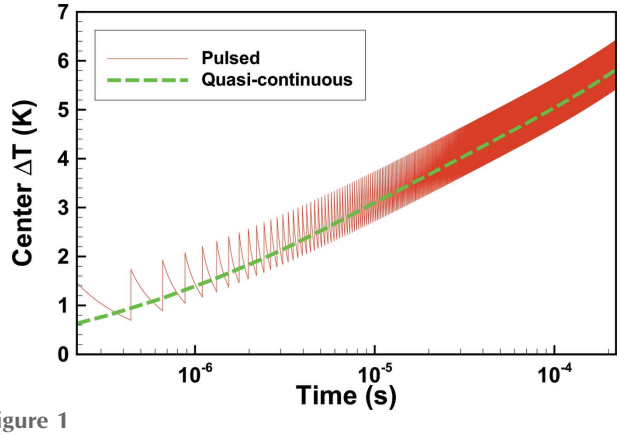

Figure 1
Temperature rise history at the center of the SASE spot. The red line represents the pulsed simulation results, while the thick dash green line shows the quasi-continuous results where the SASE pulse energy is averaged over time as indicated by Liu *et al.* (2019).

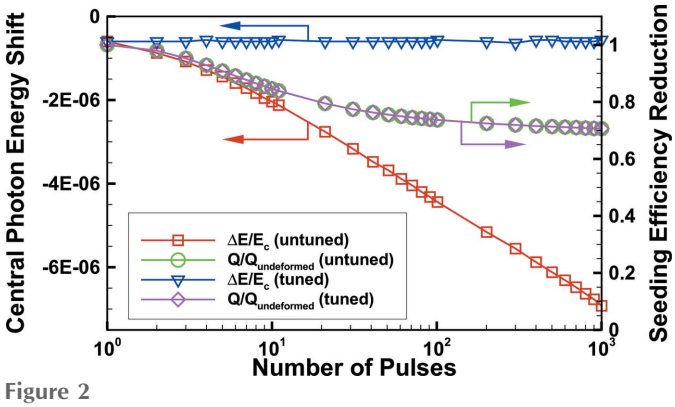

Figure 2
The seed quality degradation history due to dynamic thermal load. The red squares and green circles display the seed quality history without tuning (the crystal monochromator is fixed), while the blue triangular and violet diamond lines show the seed quality history with tuning (the crystal monochromator pitch angle is changing following the tuning curve).

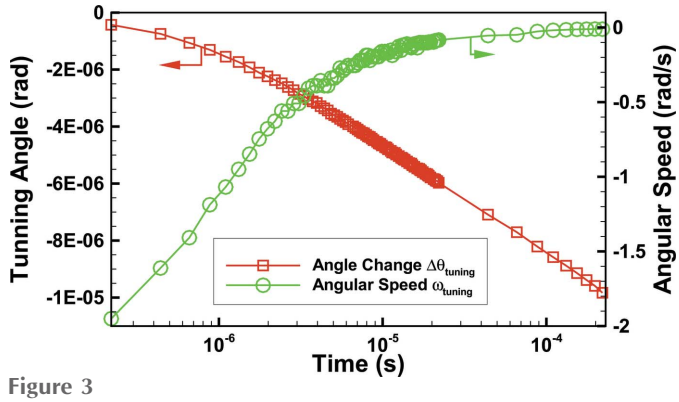

Figure 3
The tuning pitch angle change and corresponding angular speed for the motor with time. The red squares are the tuning pitch angle change, while the green circles are the angular speed.

seeding efficiency decrease as more pulses passing through the crystal. After 1000 shots, the seed central energy shifts outside the half Darwin width [half of the relative bandwidth 1.36×10^{-5} (Liu *et al.*, 2019)], and the seeding efficiency decreases to about 70% of its original value (when the crystal is not deformed). The seed bandwidth is not significantly affected because the spectral transmission curve is not significantly distorted from a rectangular function shape, so it is not discussed in this study. More details of the generation of the wake seed can be found in the book by Geloni (Geloni, 2016).

The decrease of the seed central photon energy is due to the lattice thermal expansion (strain $\varepsilon > 0$), as explained by the differential form of Bragg condition

$$-\frac{\delta E}{E} = \frac{\delta d}{d} + \cot\theta\,\delta\theta, \tag{1}$$

where E is the photon energy, d is the interplanar distance and θ is the glancing angle of the SASE pulse. If strain $\varepsilon \equiv (\delta a)/a = (\delta d)/d > 0$, then $(\delta E)/E < 0$ and the central photon energy decreases.

On the other hand, the reduction of the seeding efficiency is attributed to the non-uniformity of the strain (ε) and surface slope ($\delta\theta$) field within the SASE footprint. A more explicit explanation based on equation (1) is that $(\delta E)/E$ varies for different locations inside the spot if the strain and surface slope field are non-uniform. For example, within the footprint (3σ range) on the top surface, the maximal and minimal strain is 6.5×10^{-6} and 4.3×10^{-6}. Therefore, the overall spectral transmission curve, which is a weighted average of all different locations, will be broadened, leading to the reduction of the seed quality.

Based on the curves in Fig. 2, the tuning process can be employed if one is able to vary the angle between the crystal and the XFEL. By introducing a pitch angle change, $\delta\theta_{\rm tuning}$, we can rewrite equation (1) and set it to be zero,

$$-\frac{\delta E}{E} = \frac{\delta d}{d} + \cot\theta\,(\delta\theta + \delta\theta_{\rm tuning}) = 0. \tag{2}$$

By solving equation (2), we obtain the required glancing angle change ($\delta\theta_{\rm tuning}$) and corresponding angular speed of the motor ($\omega_{\rm tuning}$) to keep the seed central photon energy from shifting, as plotted in Fig. 3. The pitch angle should be adjusted smaller in an approximately logarithmic manner due to the mathematical form (harmonic series) of the temperature evolution (Qu *et al.*, 2020*b*), which requires the motor to provide angular speed also in a logarithmic manner.

With tuning, the seed quality is re-evaluated and plotted in Fig. 2 as the blue triangles and violet diamonds. The seed central photon energy shift is successfully eliminated, as indicated by the flat blue curve on the top. However, the seeding efficiency does not recover to its original value and still behaves in the same pattern as that in the untuned case. This is because tuning the crystal pitch angle does not refrain the non-uniformity of the strain and surface slope field within the SASE footprint.

The elimination of the seed central photon energy shift is very important and beneficial to many photon science experiments. It is also very important for cascade systems with multiple monochromators: if the spectral transmission curves mismatch between different monochromators, there could be significantly increased thermal load on the downstream monochromator, or there could be no detectable seed generated from the downstream monochromators. On the other hand, the seeding efficiency reduction could also be a severe issue since the self seeding could not work if the seed cannot remain dominant over the noise.

4. Conclusions

In this study, we simulated the dynamic pulse-to-pulse thermal load in pulse train mode and evaluated the dynamic seed quality degradation as a function of number of pulses. Our results indicate that a quasi-steady state was not reached under the specified conditions. Both seed central photon energy and seeding efficiency decrease throughout the simulated 1000 pulses. Based on the simulation, we extracted the pitch angle tuning curve and show that the seed central photon energy can be tuned back. However, the seed efficiency degradation cannot be tuned back in this method.

Acknowledgements

This work was supported by the National Science Foundation (#1637370) and the US Department of Energy (DE-AC02-76SF00515 and Office of Science Early Career Research Program grant FWP-20l3-SLAC-100l64). The authors thank T.O. Raubenheimer, M. Rowen, D. Zhu, J. Kryzwinski, Y. Feng, L. Zhang, F.-J. Decker, A. A. Lutman, H.-D. Nuhn, J. Welch, Z. Huang of SLAC, M. Yabashi, T. Osaka of SAC LA, H.-S. Kang, I. Nam, G. Kim of PAL-XFEL, H. Sirm, J. Gruenert, S. Liu, S. Serkez, J. Liu of EuXFEL for stimulating discussions.

Funding information

Funding for this research was provided by: US Dependent of Energy (contract No. DE-AC02-76SF00515; grant No. FWP-2013-SLAC-100164); National Science Foundation (grant No. 1637370).

References

Amann, J., Berg, W., Blank, V., Decker, F., Ding, Y., Emma, P., Feng, Y., Frisch, J., Fritz, D., Hastings, J., Huang, Z., Krzywinski, J., Lindberg, R., Loos, H., Lutman, A., Nuhn, H., Ratner, D., Rzepiela, J., Shu, D., Shvyd'ko, Y., Spampinati, S., Stoupin, S., Terentyev, S., Trakhtenberg, E., Walz, D., Welch, J., Wu, J., Zholents, A. & Zhu, D. (2012). *Nat. Photon.* **6**, 693–698.

Andruszkow, J., Aune, B., Ayvazyan, V., Baboi, N., Bakker, R., Balakin, V., Barni, D., Bazhan, A., Bernard, M., Bosotti, A., Bourdon, J. C., Brefeld, W., Brinkmann, R., Buhler, S., Carneiro, J., Castellano, M., Castro, P., Catani, L., Chel, S., Cho, Y., Choroba, S., Colby, E. R., Decking, W., Den Hartog, P., Desmons, M., Dohlus, M., Edwards, D., Edwards, H. T., Faatz, B., Feldhaus, J., Ferrario, M., Fitch, M. J., Flöttmann, K., Fouaidy, M., Gamp, A., Garvey, T., Gerth, C., Geitz, M., Gluskin, E., Gretchko, V., Hahn, U., Hartung, W. H., Hubert, D., Hüning, M., Ischebek, R., Jablonka, M., Joly, J. M., Juillard, M., Junquera, T., Jurkiewicz, P., Kabel, A., Kahl, J., Kaiser, H., Kamps, T., Katelev, V. V., Kirchgessner, J. L., Körfer, M., Kravchuk, L., Kreps, G., Krzywinski, J., Lokajczyk, T., Lange, R., Leblond, B., Leenen, M., Lesrel, J., Liepe, M., Liero, A., Limberg, T., Lorenz, R., Hua, L. H., Hai, L. F., Magne, C., Maslov, M., Materlik, G., Matheisen, A., Menzel, J., Michelato, P., Möller, W., Mosnier, A., Müller, U., Napoly, O., Novokhatski, A., Omeich, M., Padamsee, H. S., Pagani, C., Peters, F., Petersen, B., Pierini, P., Pflüger, J., Piot, P., Phung Ngoc, B., Plucinski, L., Proch, D., Rehlich, K., Reiche, S., Reschke, D., Reyzl, I., Rosenzweig, J., Rossbach, J., Roth, S., Saldin, E. L., Sandner, W., Sanok, Z., Schlarb, H., Schmidt, G., Schmüser, P., Schneider, J. R., Schneidmiller, E. A., Schreiber, H., Schreiber, S., Schütt, P., Sekutowicz, J., Serafini, L., Sertore, D., Setzer, S., Simrock, S., Sonntag, B., Sparr, B., Stephan, F., Sytchev, V. A., Tazzari, S., Tazzioli, F., Tigner, M., Timm, M., Tonutti, M., Trakhtenberg, E., Treusch, R., Trines, D., Verzilov, V., Vielitz, T., Vogel, V., Walter, G., **v**, Wanzenberg, R., Weiland, T., Weise, H., Weisend, J., Wendt, M., Werner, M., White, M. M., Will, I., Wolff, S., Yurkov, M. V., Zapfe, K., Zhogolev, P. & Zhou, F. (2000). *Phys. Rev. Lett.* **85**, 3825–3829.

Bonifacio, R., Pellegrini, C. & Narducci, L. (1984). *Opt. Commun.* **50**, 373–378.

Dong, X., Geloni, G., Karabekyan, S., Samoylova, L., Serkez, S., Sinn, H., Decking, W., Engling, C., Golubeva, N., Kocharyan, V., Krause, B., Lederer, S., Liu, S., Petrov, A., Saldin, E., Wohlenberg, T., Shu, D., Blank, V. & Terentiev, S. (2017). *38th International Free-Electron Laser Conference (FEL 2017)*, 20–25 August 2017, p. 42.

Emma, P., Akre, R., Arthur, J., Bionta, R., Bostedt, C., Bozek, J., Brachmann, A., Bucksbaum, P., Coffee, R., Decker, F.-J., Ding, Y., Dowell, D., Edstrom, S., Fisher, A., Frisch, J., Gilevich, S., Hastings, J., Hays, G., Hering, P., Huang, Z., Iverson, R., Loos, H., Messerschmidt, M., Miahnahri, A., Moeller, S., Nuhn, H.-D., Pile, G., Ratner, D., Rzepiela, J., Schultz, D., Smith, T., Stefan, P., Tompkins, H., Turner, J., Welch, J., White, W., Wu, J., Yocky, G. & Galayda, J. (2010). *Nat. Photon.* **4**, 641.

Emma, P., Frisch, J., Huang, Z., Marinelli, A., Maxwell, T., Loos, H., Nosochkov, Y., Raubenheimer, T., Welch, J., Wang, L., Woodley, M., Saini, A., Solyak, N., Qiang, J. & Venturini, M. (2014). *Proceedings of the 36th International Free-Electron Laser Conference (FEL2014)*, 25–29 August 2014, Basel, Switzerland, p. 743.

Geloni, G. (2016). *Self-Seeded Free-Electron Lasers*, pp. 161–193. Switzerland: Springer International Publishing.

Geloni, G., Kocharyan, V. & Saldin, E. (2011). *J. Mod. Opt.* **58**, 1391–1403.

Inoue, I., Osaka, T., Hara, T., Tanaka, T., Inagaki, T., Fukui, T., Goto, S., Inubushi, Y., Kimura, H., Kinjo, R., *et al.* (2019). *Nat. Photon.* **13**, 319–322.

Ishikawa, T., Aoyagi, H., Asaka, T., Asano, Y., Azumi, N., Bizen, T., Ego, H., Fukami, K., Fukui, T., Furukawa, Y., Goto, S., Hanaki, H., Hara, T., Hasegawa, T., Hatsui, T., Higashiya, A., Hirono, T., Hosoda, N., Ishii, M., Inagaki, T., Inubushi, Y., Itoga, T., Joti, Y., Kago, M., Kameshima, T., Kimura, H., Kirihara, Y., Kiyomichi, A., Kobayashi, T., Kondo, C., Kudo, T., Maesaka, H., Maréchal, X. M., Masuda, T., Matsubara, S., Matsumoto, T., Matsushita, T., Matsui, S., Nagasono, M., Nariyama, N., Ohashi, H., Ohata, T., Ohshima, T., Ono, S., Otake, Y., Saji, C., Sakurai, T., Sato, T., Sawada, K., Seike, T., Shirasawa, K., Sugimoto, T., Suzuki, S., Takahashi, S., Takebe, H., Takeshita, K., Tamasaku, K., Tanaka, H., Tanaka, R., Tanaka, T., Togashi, T., Togawa, K., Tokuhisa, A., Tomizawa, H., Tono, K., Wu, S., Yabashi, M., Yamaga, M., Yamashita, A., Yanagida, K., Zhang, C., Shintake, T., Kitamura, H. & Kumagai, N. (2012). *Nat. Photon.* **6**, 540–544.

Kang, H., Min, C., Heo, H., Kim, C., Yang, H., Kim, G., Nam, I., Baek, S. Y., Choi, H., Mun, G., Park, B. R., Suh, Y. J., Shin, D. C., Hu, J., Hong, J., Jung, S., Kim, S., Kim, K., Na, D., Park, S. S., Park, Y. J., Han, J., Jung, Y. G., Jeong, S. H., Lee, H. G., Lee, S., Lee, S., Lee, W., Oh, B., Suh, H. S., Parc, Y. W., Park, S., Kim, M. H., Jung, N., Kim, Y., Lee, M., Lee, B., Sung, C., Mok, I., Yang, J., Lee, C., Shin, H., Kim, J. H., Kim, Y., Lee, J. H., Park, S., Kim, J., Park, J., Eom, I., Rah, S., Kim, S., Nam, K. H., Park, J., Park, J., Kim, S., Kwon, S., Park, S. H., Kim, K. S., Hyun, H., Kim, S. N., Kim, S., Hwang, S., Kim, M. J., Lim, C., Yu, C., Kim, B., Kang, T., Kim, K., Kim, S., Lee, H., Lee, H., Park, K., Koo, T., Kim, D. & Ko, I. S. (2017). *Nat. Photon.* **11**, 708–713.

Kondratenko, A. & Saldin, E. (1980). *Part. Accel.* **10**, 207–216.

Liu, S., Decking, W., Kocharyan, V., Saldin, E., Serkez, S., Shayduk, R., Sinn, H. & Geloni, G. (2019). *Phys. Rev. Accel. Beams*, **22**, 060704.

Milathianaki, D., Boutet, S., Williams, G. J., Higginbotham, A., Ratner, D., Gleason, A. E., Messerschmidt, M., Seibert, M. M., Swift, D. C., Hering, P., Robinson, J., White, W. E. & Wark, J. S. (2013). *Science*, **342**, 220–223.

Qu, Z. (2020). *Photo-Thermo-Mechanical Analysis and Control for High-Brightness and High-Repetition-Rate X-ray Optics.* PhD thesis, University of California Merced, California, USA.

Qu, Z., Ma, Y., Zhou, G. & Wu, J. (2020*a*). *Nucl. Instrum. Methods Phys. Res. A*, **969**, 163936.

Qu, Z., Ma, Y., Zhou, G. & Wu, J. (2020*b*). *Opt. Express*, **28**, 30075.

Raubenheimer, T. (2016). *Workshop on Scientific Opportunities for Ultrafast Hard X-rays at High Repetition Rate*, 26–27 September 2016, SLAC, USA.

Raubenheimer, T. (2014). *Proceedings of the 36th International Free-Electron Laser Conference (FEL2014)*, 25–29 August 2014, Basel, Switzerland. Presentation No. WEB01.

Raubenheimer, T. (2018). *Proceedings of the 60th ICFA Advanced Beam Dynamics Workshop (FLS'18)*, 5–9 March 2018, Shanghai, China, pp. 6–11. MOP1WA02 (http://jacow.org/fls2018/papers/mop1wa02.pdf).

Samoylova, L., Shu, D., Dong, X., Geloni, G., Karabekyan, S., Terentev, S., Blank, V., Liu, S., Wohlenberg, T., Decking, W. & Sinn, H. (2019). *AIP Conf. Proc.* **2054**, 030016.

Scholz, M. (2018). *Proceedings of the 9th International Particle Accelerator Conference (IPAC2018)*, 29 April–4 May 2018, Vancouver, BC, Canada, p. 29.

Seibert, M. M., Ekeberg, T., Maia, F. R. N. C., Svenda, M., Andreasson, J., Jönsson, O., Odić, D., Iwan, B., Rocker, A., Westphal, D., Hantke, M., DePonte, D. P., Barty, A., Schulz, J., Gumprecht, L., Coppola, N., Aquila, A., Liang, M., White, T. A., Martin, A., Caleman, C., Stern, S., Abergel, C., Seltzer, V., Claverie, J.-M., Bostedt, C., Bozek, J. D., Boutet, S., Miahnahri, A. A., Messerschmidt, M., Krzywinski, J., Williams, G., Hodgson, K. O., Bogan, M. J., Hampton, C. Y., Sierra, R. G., Starodub, D., Andersson, I., Bajt, S., Barthelmess, M., Spence, J. C. H., Fromme, P., Weierstall, U., Kirian, R., Hunter, M., Doak, R. B., Marchesini, S., Hau-Riege, S. P., Frank, M., Shoeman, R. L., Lomb, L., Epp, S. W., Hartmann, R., Rolles, D., Rudenko, A., Schmidt, C., Foucar, L., Kimmel, N., Holl, P., Rudek, B., Erk, B., Hömke, A., Reich, C., Pietschner, D., Weidenspointner, G., Strüder, L., Hauser, G., Gorke, H., Ullrich, J., Schlichting, I., Herrmann, S., Schaller, G., Schopper, F., Soltau, H., Kühnel, K.-U., Andritschke, R., Schröter, C.-D., Krasniqi, F., Bott, M., Schorb, S., Rupp, D., Adolph, M., Gorkhover, T., Hirsemann, H., Potdevin, G., Graafsma, H., Nilsson, B., Chapman, H. N. & Hajdu, J. (2011). *Nature*, **470**, 78–81.

Shvyd'ko, Y. & Lindberg, R. (2012). *Phys. Rev. ST Accel. Beams*, **15**, 100702.

Wu, J., Ding, Y., Emma, P., Huang, Z., Loos, H., Messerschmidt, M., Schneidmiller, E. & Yurkov, M. (2010). *Proceedings of the 32nd International Free Electron Laser Conference (FEL2010)*, Malmo, Sweden, 23–27 August 2010, p. 147 (http://accelconf.web.cern.ch/AccelConf/FEL2010/papers/mopc14.pdf).

Young, L., Kanter, E. P., Krässig, B., Li, Y., March, A., Pratt, S., Santra, R., Southworth, S., Rohringer, N., DiMauro, L., Doumy, G., Roedig, C. A., Berrah, N., Fang, L., Hoener, M., Bucksbaum, P. H., Cryan, J. P., Ghimire, S., Glownia, J. M., Reis, D. A., Bozek, J. D., Bostedt, C. & Messerschmidt, M. (2010). *Nature*, **466**, 56–61.

Zhang, W., Alonso-Mori, R., Bergmann, U., Bressler, C., Chollet, M., Galler, A., Gawelda, W., Hadt, R. G., Hartsock, R. W., Kroll, T., Kjaer, K. S., Kubiček, K., Lemke, H. T., Liang, H. W., Meyer, D. A., Nielsen, M. M., Purser, C., Robinson, J. S., Solomon, E. I., Sun, Z., Sokaras, D., van Driel, T. B., Vankó, G., Weng, T. C., Zhu, D. & Gaffney, K. J. (2014). *Nature*, **509**, 345–348.

Zhou, G., Jiao, Y., Raubenheimer, T., Tsai, C.-Y., Wang, J., Wu, J. & Yang, C. (2019). *Proceedings of the 10th International Particle Accelerator Conference (IPAC2019)*, 19–24 May 2019, Melbourne, Australia, p. 1820–1823. TUPRB062.